Journal Name

ARTICLE

Supplementary material

Absorption spectroscopy of the oxidized scintillator

The scintillator liquid not only has to remain fluorescent but it also has to be transparent over a length of at least 12 m. The same samples that were prepared by heating the SNO+ scintillator replica to different high temperatures under breathing grade air, and that were analysed using EEM spectroscopy, were also subjected to absorption measurements.

As observed in **Figure 3** in the main text, the scintillation replica when heated and exposed to breathing grade air quickly transforms from a transparent to an opaque black solution. **Figure S1(a)** shows the absorption spectra for the oxidized solution at 466 K. As expected the absorption increases as the solution is aged. The absorption peak also shifts to longer wavelengths as the reaction proceeds. The absorption spectra of neat PPO and bis-MSB in LAB (**Figure S1(b)**) agree well with the integrated fluorescence excitation spectra of the corresponding PARAFAC components (**Figure S1(d)**). PARAFAC analysis on the 74 absorption spectra of the heated samples (67 oxidized, 7 inert) yields spectra of two distinct components, AO1 and AO2 (**Figure S1(b)**). Component AO2 can be unambiguously associated with the PPO absorption spectrum. Bis-MSB is present at only 15 mg/L (0.048 mmol/L) and could not be identified in the absorption spectra, likely because it is far less concentrated than PPO at 2 g/L (9 mmol/L). The absorption component AO1 shows a peak located at 280 nm (**Figure S1(c)**), which matches the small peak in the F2 (bis-MSB) excitation spectrum in **Figure S1(d)**. Absorption around 280 nm is frequently caused by phenyl groups. The red-shifted absorption in AO1 corresponds to

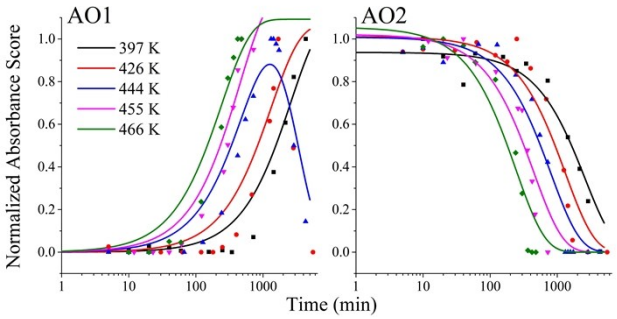

Figure S2: Normalized scores of the two components obtained by PARAFAC analysis of the absorption spectra of the 74 heated samples (67 oxidized, 7 inert). The lines represent fits through the data using equations 8 and 4. Only the 444 K data series was fit to equation 9 as this was the only one with enough data points showing a clear maximum.

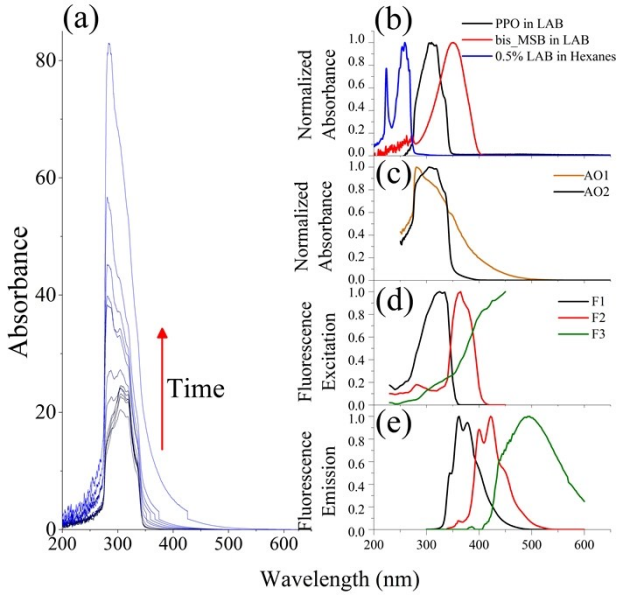

Figure S1: (a) Absorbance spectra for the 455 K heated with air series using a 1 mm cuvette. As the sample is aged the absorbance increases. (b) normalized absorption spectra of PPO in LAB, bis-MSB in LAB and 0.5% LAB diluted in hexanes (c) normalized absorbance spectra of the 2 components (AO1, AO2) found using PARAFAC on the 74 heated samples (67 oxidized, 7 inert) are given. (d) normalized fluorescence excitation and (e) fluorescence emission spectra of F1 (PPO), F2 (bis-MSB) and F3 (bis-MSB product).

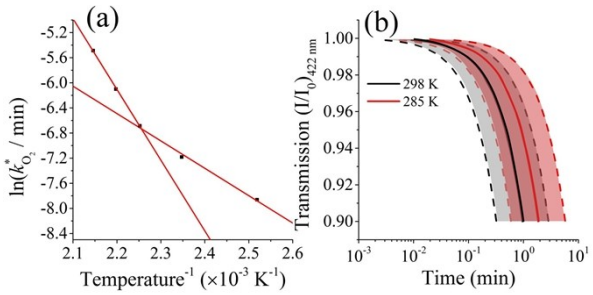

Figure S3: (a) Arrhenius plot using the rate constants, $k^*_{O_2}$, obtained from the exponential rise and decay fits in **Figure S2**. The slope at lower temperatures gives the activation energy of Component AO1 and AO2, as 36.2 ± 2.7 kJmol^{-1}, which matches the activation energy of F1 (PPO). The slope at hotter temperatures gives an activation energy of 93.7 ± 2.7 kJmol^{-1} (b) The predicted transmission I/I_0 as the solution degrades at 298 and 285 K using the predicted rates obtained using the activation energies obtained in **Figure S3(a)** and a maximum pathlength in the SNO+ vial of 12 m. The shaded area between the dashed lines represent the upper and lower boundary using one standard deviation of the activation energy.

Table S1: Rate constants for the decay and rise of absorbance components AO1 and AO2 in figure S2. The temperatures marked with a # are extrapolated rate constants obtained from the activation energy determined at lower temperatures from the linear fit in figure S3(a).

	Temperature (K)							E_a < 444 K [kJ mol^{-1}]	E_a > 444 K [kJ mol^{-1}]	A < 444 K [min^{-1}]	A > 444 K [min^{-1}]
	285#	298#	397	427	444	455	466				
$k^*_{O_2}$ (AO1, AO2) (×10^{-3} min^{-1})	0.0051	0.0099	0.385	0.760	1.25	2.24	4.14	36.2 (2.7)	93.7 (2.5)	22.2 (5.5)	1.298 (0.047) x10^8

more conjugated products such as dimers or oligomers as mentioned in section 3. These products may include the bis-MSB product apparent in the fluorescence excitation spectrum of **Figure S1(d)** or products of PPO degradation. A more thorough analysis of the by-products is outside the scope of this paper.

The absorption scores obtained by PARAFAC analysis of the 67 oxidized samples are given in **Figure S2**. The scores for the 7 thermally aged samples under inert atmosphere were excluded as they showed no degradation. Component AO1 increases and decays as the SNO+ replica reacts with O_2 and the scores of this PARAFAC component fit quite well to equation * MERGEFORMAT (8). For most temperatures, there were not enough data on the decreasing slope and only the rate constant associated with the rise was found. Component AO2, which rapidly decays under the influence of O_2, shows a single exponential decay and fits well to equation * MERGEFORMAT (4). Both components AO1 and AO2 were fit to the same rate constants given in **Table S1**.

As with the fluorescence data, the rates determined by the fits of the scores can serve to obtain activation energies. **Figure S3(a)**. Using the Arrhenius plot the activation energy for the decay of AO2 and formation of AO1 was found to be 36.2 ± 2.7 kJmol^{-1} at lower temperatures. This matches the activation energy of PPO degradation as obtained by the fluorescence. Thus AO1 is likely the absorption of the PPO product. At higher temperatures the activation energy is 93.7 ± 2.5 kJmol^{-1}. This appearance of a kink in the Arrhenius plot is unusual. However, components AO1 and AO2 are related to absorption and it is likely that at higher temperatures, additional products from the degradation of PPO, bis-MSB, and LAB in addition to further sequential product formation will contribute to this increase in absorption. Components AO2 and, especially, AO1, also incorporate these breakdown products at higher temperatures and deviate further from describing solely the degradation of PPO and the formation of one of its product. This explains why the fits to the data in Figure **S2** are less than ideal.

Figure S3(b) shows the predicted transmission of light through the SNO+ detector. As shown, the transmission of light through the SNO+ detector will fall to 90% (99%) in 140 min (13 min) at 285 K in the presence of oxygen (mole fraction of 3.2-5.3×10^{-4}). Again, reducing the concentration of oxygen in the scintillation solution will increase its lifetime. Reducing the partial pressure of O_2 in the headspace to 4.2×10^{-3} Pa (41 ppb$_v$), which is a dissolved mole fraction of O_2 to 1.13-1.9×10^{-10} (14-23 ppt$_w$) will ensure the solution will remain 90% transparent over 7 years. Given that the Arrhenius plot does not show a single decay process, and that the activation energies and rate constants are a rather ambiguous guess, these estimates are a lot less reliable compared to those obtained from fluorescence EEM spectroscopy.

In general, we found that rate measurements that are based on the formation rates of products tend to be less reliable than those obtained from the depletion of (fluorescent) reactants.